Chapter 7

MEMS inertial sensors

7.1 Introduction

New applications that have demanded low-cost sensors for providing measurements of acceleration and angular motion have provided a major incentive for the development of micro-machined electromechanical system (MEMS) sensors. One typical modern application is the use of inertial sensors in transport, such as motor cars; an indication of the current extent of the use of these devices in this application and examples of many others are given in Chapter 15.

MEMS devices are one of the most exciting developments in inertial sensors in the last 25 years. These devices overcome many of the features that have impeded the adoption of inertial systems by many potential applications, especially where cost, size and power consumption have been governing parameters. Many efforts involving value engineering and automation have been applied to the design and manufacture of conventional inertial instruments, with significant success; however, the cost has remained high. The major reasons centre on:

- high parts count;
- requirement for many parts with high-precision tolerances;
- intricate and precision assembly techniques;
- accurate testing, characterisation and calibration.

The use of silicon as the base material in the manufacture of the components offers a radical approach and overcomes many of the issues considered above for conventional mechanical sensors. This is summarised in Figure 7.1. Additionally, they can be considered as offering a sensing device on a chip with the very real prospect of a precision inertial measurement unit sensor on a chip in the near future. This holds the opportunity to make an inertial navigation system (with GPS aiding) costing less than $1000.

MEMS sensor technology makes direct use of the chemical etching and batch processing techniques used by the electronics integrated circuit industry. Precision

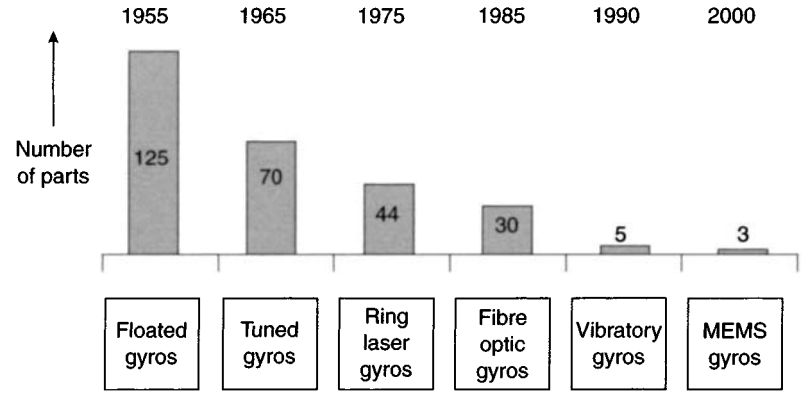

Figure 7.1 Reduction in part count

techniques developed by this industry for 'machining silicon' have been adapted to make very small mechanical structures using silicon or quartz. Particular advances have been obtained through the use of plane-wall etching. The properties of the resulting solid-state sensors, viz.

- small size;
- low weight;
- rugged construction;
- low power consumption;
- short start-up time;
- inexpensive to produce (in high volume);
- high reliability;
- low maintenance;
- compatible with operation in hostile environments;

provide the engineer with a level of design flexibility beyond anything that has preceded these developments. The consequence has been a proliferation of applications, both military and commercial, where such devices may be used; some of these are discussed in Chapter 15.

The properties of silicon and the ease of perfecting high-fidelity components was a key breakthrough in the transition of this sensor technology from a research device to a practical, mass–volume sensor. However, the reduction in size of the sensing elements brings with it challenges for attaining good measurement performance and high resolution. In general, reductions in size give rise to decreases in sensitivity/scale-factor and increases in noise. In addition, there are thermal sensitivity concerns; for example, the change in the Young's modulus of silicon with temperature is $\sim$100 ppm/°C.

Despite these limitations, low-cost MEMS gyroscopes and accelerometers demonstrating performance approaching 1°/h and 50–100 micro-g, respectively, are expected to become readily available within the next few years. One of the major

reasons for the enhanced performance of MEMS devices is the ability to undertake complex compensation of the systematic errors exhibited by these sensors, which can now be accomplished in real time. Complex or deep compensation methods rely on a very detailed knowledge of both the error mechanisms and the fundamental characteristics of each sensor type and have to be embodied into the design of the Kalman filter to give IMU–level compensation.

Moreover, recent research has given rise to an enhanced understanding of the physical behaviour of the sensing element technology and the fundamental interaction with the supporting electronics used by these devices. These advances, along with sophisticated compensation techniques, have seen a dramatic increase in the measurement accuracy. Over the last decade techniques have been demonstrated that will enable the measurement accuracy of the best quality devices to approach those of inertial-grade sensors, namely:

- angular rate measurement accuracy of 0.01°/h with MEMS gyroscopes;
- specific force measurement to better than 1 milli-g from MEMS accelerometers.

Hence, there is the real prospect that such devices with enhanced performance will displace ring laser and fibre optic gyroscopes in many tactical applications in a similar time scale.

Initial MEMS sensor developments focused on the generation of miniature accelerometers, the system and performance requirements of which were driven by the demands of the automobile industry. As a result, MEMS accelerometer technology was the first to achieve a level of technical maturity, with a significant number of sensors now being commercially available.

In contrast, there was less of a stimulus for the development of similar angular measurement sensors, so commercially available devices in this class were slow to emerge initially. More recently, MEMS gyroscopic sensor development has been the subject of significant investment and development effort in industry and research institutions, both in Europe and the United States, culminating in the wide availability of lower cost/lower performance sensors in recent years. Research effort has concentrated, and continues to be focused, on both the physics of the devices as well as the refinement of the batch processing techniques required for their cost-effective manufacture leading to a high batch yield.

There are a number of reasons for the phenomenal increase in the performance of the sensors during the last decade of the twentieth century; particularly plane-wall etch. This has been a direct result of enhanced knowledge of the effects of geometry of the structure and its size, as well as the electronics and packaging, on the ultimate performance and reliability of the devices. Moreover, there has been a significant investment in developing techniques for integrating all of the sensors on to a single chip, which led to many system and performance benefits.

Hence these micro-miniature devices appear to be the sensors of the future. This is because they are based on a solid-state architecture and with careful design have few components and therefore have the potential to become the 'Holy Grail' for inertial sensor technology. Consequently, inertial sensor technology developments in recent

years have been concentrated almost exclusively on the development and perfection of MEMS devices.

In the more distant future it is likely that further enhancements in performance could show a similar trend. The miniature sensors of the future may well be based on micro-opto-electromechanical systems (MOEMS). Currently, the technology required to make a true MOEMS device with an optical read-out has not been reported.

This chapter sets out to summarise the advances in MEMS technology relating to sensors designed to measure both angular rotation and linear acceleration. The physical principles of the operation of these devices are considered along with an attempt to predict the future technical performance of these devices.

7.2 Silicon processing

The use of silicon to make the sensing elements is attractive, as it is a proven route to cost reduction through use of techniques developed in the semiconductor electronics industry for wafer processing. This industry has established very effective robust methods for high-yield and high-volume production that lead to precision low-cost components. Moreover, the mechanical properties of crystalline silicon are interesting as it has a fracture limit of 7 GPa, which exceeds that of many steel alloys; additionally, its density is quite low at 2390 kg/m^3. Hence, crystalline silicon is very robust and ideal for this application.

A range of manufacturing techniques has been devised and perfected over the last three or four decades. These have concentrated on rapid and accurate etching approaches that avoid mechanical methods such as sawing, cleaving or filing. The modern methods lead to components with flat surfaces and an absence of undercutting. Efficient chemical 'machining' methods are very attractive, as they enable stress-free components to be produced rapidly. Moreover, the technique is capable of producing multiple components with identical dimensions to a high tolerance and having identical characteristics.

Silicon processing enables a robust design process to be devised. It is possible to reduce the fabrication process to three mask levels. For example, a 100 μm wafer can have a deposited oxide layer patterned with mask level 1, with a metal layer sputter deposited and patterned with mask level 2. Finally, photo-resist is spun and patterned with mask level 3 giving the shape of the resonator structure that is then generated through a dry deep-trench etch technique. On completion of the etching process the photo-resist is removed leaving a wafer of resonators.

The silicon wafer of resonators is anodically bonded to a pre-shaped glass wafer and then diced to give individual sensor elements. This design technique avoids the need to leave small gaps between the resonator and the surrounding material required for conventional processing; consequently the problems associated with stiction are mitigated. Additionally with some designs, such as the ring resonator where the vibratory motion is in one plane, all of the silicon processing is planar, thus avoiding the necessity for multi-layer processing.

Trade-off studies have shown that optimal gyroscopic performance is achieved with sensing elements having a thickness in the region of 50–100 μm. It is considered

that continued evolution of the advanced micro-machining processes are required to build thicker and more three-dimensional parts that have less critical tolerances on the entire structure in order to reduce the cost of these sensors.

Another suitable material used as an alternative to crystalline silicon is quartz, and its application as the base material for MEMS inertial sensing devices is discussed later in the chapter.

7.3 MEMS gyroscope technology

7.3.1 Introduction

MEMS gyroscopes operate on a very similar principle to that already described for vibrating gyroscopes, in Chapter 4. However, it will be described again here, but in the context of a MEMS gyroscope.

MEMS gyroscopes are non-rotating devices and use the Coriolis acceleration effect on a vibrating proof mass(es) to detect inertial angular rotation. Thus, these sensors rely on the detection of the force acting on a mass that is subject to linear vibratory motion in a frame of reference which is rotating about an axis perpendicular to the axis of linear motion. The resulting force, the Coriolis force, acts in a direction, that is perpendicular to both the axis of vibration and the axis about which the rotation is applied. This is shown in Figure 7.2.

Whilst there are many practical sensor configurations based upon this principle, they fall generally into one of the three categories described below, and discussed previously in Chapter 4:

- simple oscillators;
- balanced oscillators (tuning fork gyroscope);
- shell resonators (wine glass, cylinder, ring oscillators).

Figure 7.3 provides a schematic illustration of these three angular sensors.

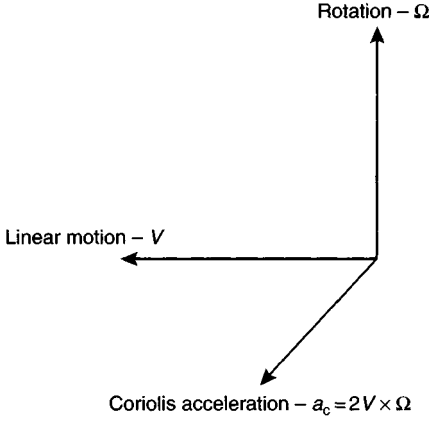

Figure 7.2 Generation of Coriolis force

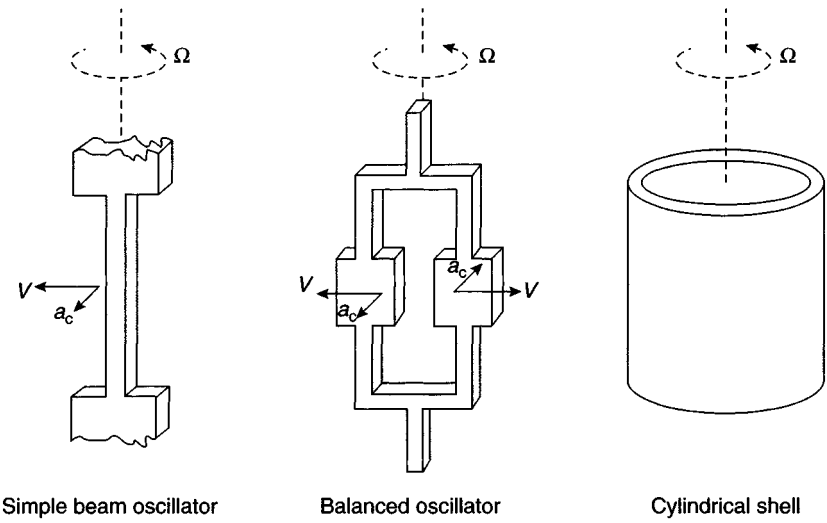

Figure 7.3 Classes of MEMS oscillator

Simple oscillators form the most basic class of vibratory gyroscopes; devices based on an oscillator that can be modelled as a single vibrating mass. The major drawbacks in this type of design arise through mechanical asymmetry, resulting in additional coupling between the axis of vibration and the output or measurement axis, and sensitivity to external vibration and interaction of the vibrating element with the structure on which the instrument is mounted. The latter effect is attributable to the reaction forces exerted by the case of the sensor on the vibrating member. One of the more successful sensor designs, which fall into this category, is the vibrating wire sensor, as described in Chapter 4 (Section 4.4.8).

The problems associated with the sensitivity simple oscillators to external vibration can be largely overcome by using a balanced oscillator. A device of this type that has received considerable attention over the years is the tuning fork gyroscope (TFG), and a number of MEMS sensors based upon this principle have been produced using either quartz or silicon in their construction. As discussed later in the chapter, it is the developments based around the TFG principle that have resulted in significant performance improvements in recent years.

The third category for this type of sensor is the vibrating shell or ring device, which is symmetric about the axis of rotation. Sensors that fall into this category include the wine glass gyroscope and devices based on a vibrating cylinder or ring. Such devices are relatively easy to manufacture to a high level of accuracy.

MEMS devices have been implemented based upon a vibrating ring structure. For such a ring, the modes of flexural vibration may be classified as in-plane or out-of-plane modes. They occur in degenerate pairs at a mutual angle of $90/p$ degrees, where p is the number of modal diameters. Existing devices measure angular rate about an axis perpendicular to the plane of the ring using the Coriolis coupling between

the in-plane modes. One mode is maintained at constant amplitude of vibration. The carrier mode may be excited by a number of methods including electromagnetic, electrostatic or piezoelectric means.

The vibrational behaviour of this type of sensor is considerably more complex than that of the simpler single mass or balanced oscillator devices outlined above. However, such devices are also less susceptible to the effects of applied vibration and the interactions between the vibrating element and the structure in which it is mounted.

As indicated above, the vibratory sensor types, which have been the focus of recent MEMS developments, have been based upon the principles of the tuning fork gyroscope and the vibrating ring device. Some examples of developments in this field of technology are described in the following sections.

7.3.2 Tuning fork MEMS gyroscopes

7.3.2.1 Silicon sensors

The focus for much of the development of advanced performance silicon tuning fork gyroscopes has been, and continues to be, The Charles Stark Draper Laboratories, Inc. in the United States. In 1992, a team of engineers succeeded in implementing a Coriolis vibratory gyroscope using MEMS technology employing silicon wafer photolithographic and chemical etching processes adapted from the electronics industry. Since that time, as part of a continuing development process, gyroscopes have been produced with an in-run bias stability in the region 3–10°/h over military operating temperatures, falling to tenths of a degree per hour in a temperature controlled environment with in-depth compensation techniques. Further dramatic improvements in performance are anticipated over the next five years.

Whilst much of this development has been directed towards military applications, driving the quest for higher performance devices, it has also been licenced for commercial exploitation. The technology lends itself to high volume, low cost production ($10 per axis) for more modest performance applications. The largest user in the near term is the automobile industry, where applications include gyroscopes for anti-skid braking, steering control, roll detection and map navigation displays.

Principles of operation

The Draper micro electromechanical gyroscope, shown in Figure 7.4, consists of a silicon structure suspended above a glass substrate. The silicon structure contains two masses suspended by a sequence of beams that are anchored to the substrate at specific points. These two masses are made to oscillate 180° out of phase through the application of voltages to the outer comb motor drives. This feature has led to the designation of the sensor as a tuning fork gyroscope; see Section 4.4.4.

The application of an angular rate about the input axis, which is perpendicular to the velocity vector of the masses, gives rise to a Coriolis force that acts to push the masses in and out of the plane of oscillation. Because the instantaneous velocity vectors of the relative masses are equal and opposite, anti-parallel motion is induced in response to the Coriolis force. The resultant motion is measured by capacitor

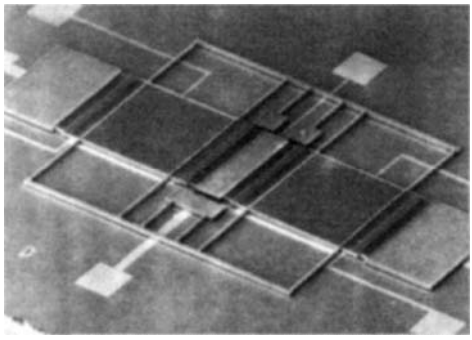

Figure 7.4 MEMS comb-drive tuning fork gyroscope (© The Charles Stark Draper Laboratory, Inc. All rights reserved. Reprinted with permission)

plates above and below each of the two masses, providing a signal proportional to the applied input rate. The operating elements of the gyroscope are shown schematically in Figure 7.5.

A simplified schematic is shown in Figure 7.6 to illustrate further the principle of operation. This diagram indicates the directions of vibration of the proof mass when the device is rotated about its input axis.

This device, also known as an in-plane sensing device,[1] is fabricated from a single crystal of silicon on Pyrex, the size of the proof mass element being $1000\,\mu m \times 1000\,\mu m \times 20\,\mu m$. The operating frequency is ~12 kHz, and the amplitude of the motion imparted to the proof mass is $10\,\mu m$ (peak). The sensor drive is electrostatic and a capacitive pick-off is employed to detect the output motion of the proof mass.

The following values are given to put into context the precision of the measurement task that needs to be undertaken in a MEMS gyroscope. For a typical device, a 1 rad/s input rate results in a Coriolis force of approximately 9×10^{-8} N, a peak motion along the sense axis of 10^{-9} m, a 3 aF (aF = attofarad; 1 aF = 10^{-18} F) peak change in capacitance and a charge generation of 15 000–65 000 electrons.

As with all gyroscopes, the design of the electronics used to drive and control the sensors is a critical sub-system. This 'component' requires careful optimisation to give stable and repeatable output, in order to achieve good and reliable performance. For the particular device described here, the drive motor loop and the sense electronics are particularly important. The motor loop comprises a self-drive oscillator that provides voltages to generate an electrostatic force to induce motion of each proof mass. This motion is sensed and controlled to sustain a constant drive amplitude. Detection of the Coriolis induced motion is carried out using a highly

[1] Care must be taken in defining what is meant by 'in-plane' and 'out-of-plane' devices. 'In-plane' refers here to the orientation of the sensitive axis of the sensor, which in this case is parallel to the plane of the sensing element. It is noted that the resulting Coriolis motion of the sensitive element is perpendicular to the plane of the device (out-of-plane).

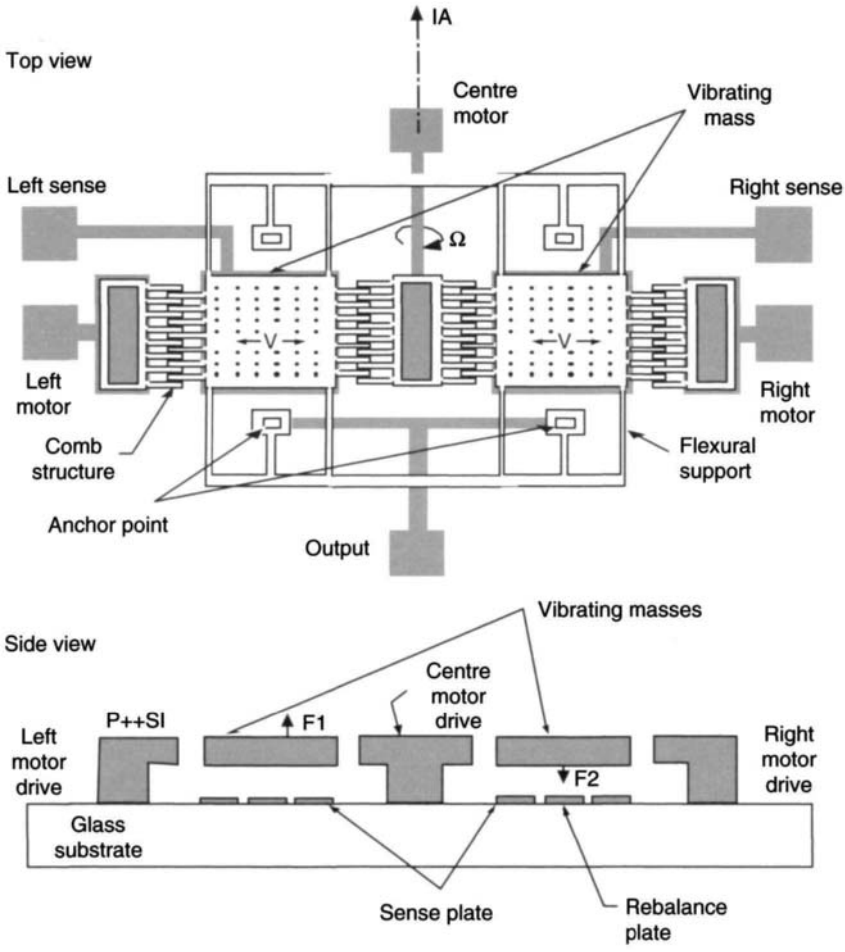

Figure 7.5 Operating elements of MEMS tuning fork gyroscope (© The Charles Stark Draper Laboratory, Inc. All rights reserved. Reprinted with permission)

sensitive capacitive pick-off. A pre-amplifier detects the charge generated through changes in proof-mass displacement. Existing devices operate in an open-loop mode, the output of the pick-off electronics providing a signal proportional to the input rate. A block diagram representation of the MEMS gyroscope electronics is given in Figure 7.7.

Sensor fabrication and packaging

Sensors are manufactured by the dissolved wafer process, illustrated in Figure 7.8. The first step (Mask 1) involves the etching of recesses in a doped-silicon wafer, which defines the height of the silicon above the glass substrate and the gap spacing

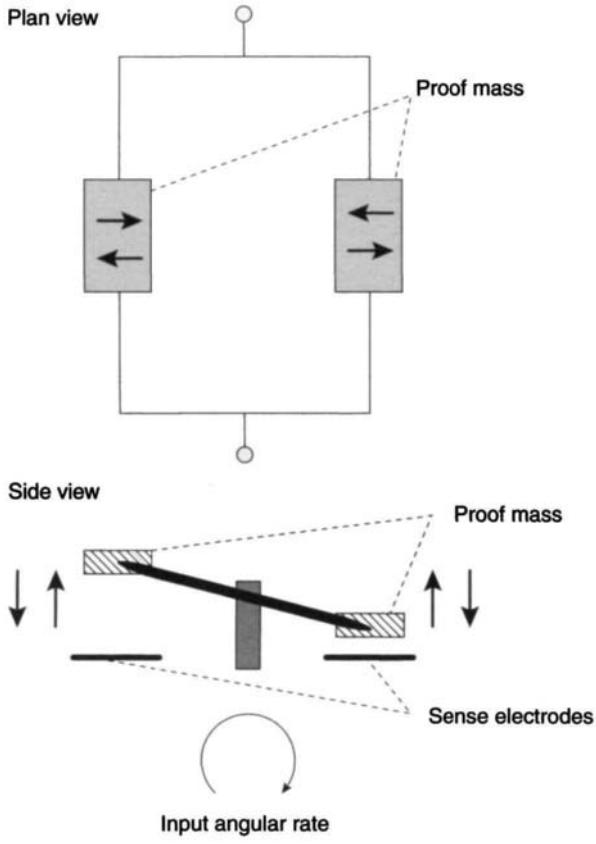

Figure 7.6 Motion of proof mass elements of a MEMS tuning fork gyroscope

for the capacitive sensing plates. A boron diffusion process follows, which defines the thickness of the structure. The pattern features are defined by Mask 2 and are then micro-machined using a reactive ion etching process. The glass wafer is processed separately, Mask 3 defining the glass recess and metal electrode pattern. The silicon wafer is then inverted and bonded to the glass wafer. This is followed by the final etching process to dissolve the un-doped silicon and leave the free-standing device. Hundreds of sensors are made on a single wafer.

The device is hermetically sealed in a package, which has a vacuum maintained in it to ensure the high-Q resonance is achieved to enable the desired operational characteristics. Leadless chip carriers (LCCs) with braze-sealed lids have been used in pilot production. Sensor chips are installed in packages using compression bonding and wire bond interconnections. The sensor package is then aligned mechanically on a printed circuit board containing the electronics. The resulting LCC is 0.25 in.^{2} by 0.1 in. high.

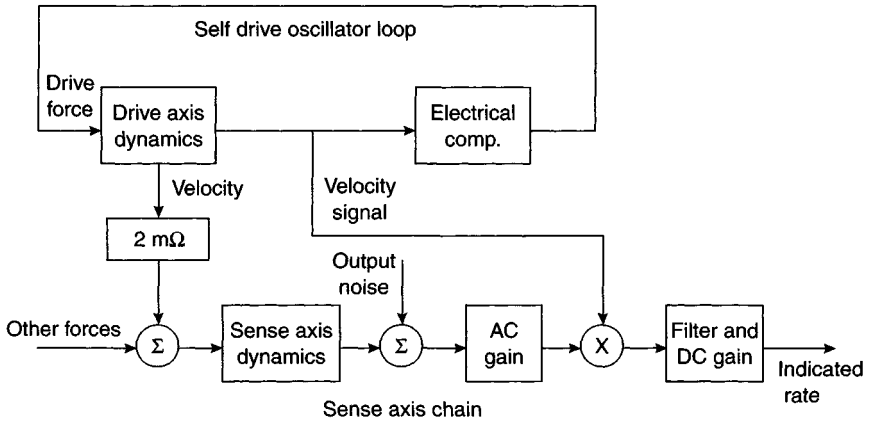

Figure 7.7 *MEMS gyroscope electronics (© The Charles Stark Draper Laboratory, Inc. All rights reserved. Reprinted with permission)*

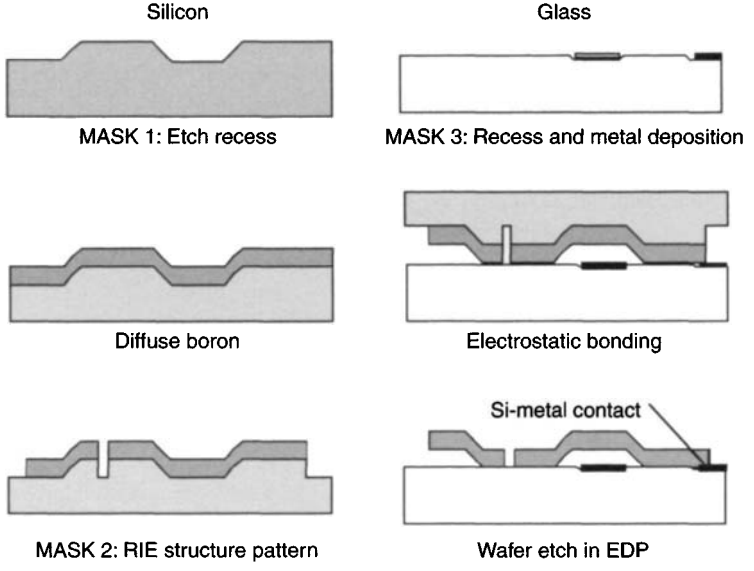

Figure 7.8 *Dissolved wafer, silicon on glass process for gyro manufacture (© The Charles Stark Draper Laboratory, Inc. All rights reserved. Reprinted with permission)*

Recent advances in the reactive ion etching process used in the manufacture of MEMS gyroscopes have resulted in designs incorporating silicon proof masses with increased component thickness up to 50 μm. The additional thickness of the silicon proof mass is expected to yield greater stability and improved device performance. In addition, recent devices include both upper and lower glass-sense plates to give

increased signal-to-noise ratio. Further details concerning the fabrication of these devices and their drive electronics can be found in the literature [1–3].

Performance

The MEMS gyroscope described here is capable of measuring rotation rates of several thousand degrees per second, whilst having the resolution to detect small fractions of a degree per hour. Typical performance figures are tabulated in Table 7.1.

It is stressed that current MEMS sensors are heavily reliant on pre-run characterisation followed by calibration to remove turn-on errors and so achieve high performance.

As with other solid-state technologies, such instruments are able to withstand high levels of mechanical shock and vibration, and hence are applicable for operation in hostile environments. MEMS gyroscopes and accelerometers have already found application in guided-munitions' applications where they must withstand and operate in the presence of launch accelerations of many thousands of *g*s. This feature combined with their capability to provide precise rotational measurements, opens up many new areas of application, many of which require in-depth investigation.

Since this is an emerging technology, it is felt to be appropriate to give some indication of performance expectations, as indicated by the performance goals given in Table 7.1. Gyroscopic performance improvements are expected to come about through the use of thicker and larger component parts; increased thickness of the silicon proof-mass in gyroscopes. This has become possible as a result of recent improvements in reactive ion etching techniques, allowing straight sidewall and flatness tolerances to be met. This in turn leads to reduced susceptibility to fabrication tolerances, higher scale-factor and greater sensor performance stability. Although higher performance

Table 7.1 MEMS tuning fork gyroscope performance figures

	Current sensors	Performance goals	Comments
Operating range (°/s)	100–6000	100–6000	Selectable
Turn-on bias stability (°/h)	10–150	<1	All environments
In-run bias stability (°/h)	3–30	<1	−40 to 85°C
	0.3–10	<0.1	5°C temperature range
Turn-on scale-factor stability (ppm)	500–1500	<100	All environments
In-run scale-factor stability (ppm)	300–1500	<100	−40 to 85°C
	100–300	<10	5°C temperature range
Angle random walk (°/$\sqrt{\text{h}}$)	0.01–0.3	0.01–0.03	Lower random walk at lower maximum input rate
g-Sensitivity (°/h/*g*)	10	0.5	

devices will be physically larger as a result of the developments outlined above, these changes will yield sensors that are still quite small in size and capable of fulfilling size requirements for the types of application in which they are expected to be used.

7.3.2.2 Quartz sensors

A number of MEMS gyroscopes use quartz as the base material for the sensing element. The use of piezoelectric quartz material simplifies the sensing element, resulting in a reliable and durable sensor that is stable over both temperature and time.

An example of this type of device is the quartz rate sensor (QRS) produced by the Systron Donner Inertial Division of BEI Technologies, Inc. [4], and described earlier in Section 4.4.5. A picture of this device, which is based around an H-shaped quartz crystal, is shown in Figure 7.9. MEMS versions of these devices are in high volume production for automobile applications, as well as uses in platform stabilisation and smart munitions; a high-g version has been produced for the latter application.

This device comprises a pair of coupled tuning forks, the drive tines and the pick-up tines, along with their support flexures and frames that are batch fabricated from thin wafers of single-crystal piezoelectric quartz. The piezoelectric drive tines are driven by an oscillator to vibrate at a precisely defined amplitude, causing the tines to move toward and away from one another at a high frequency. This vibration causes the drive fork to become sensitive to angular rate about an axis parallel to its tines, defining the true input axis of the sensor.

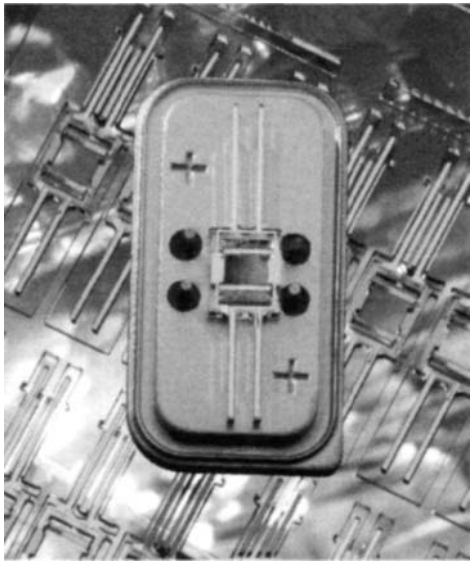

Figure 7.9 Quartz rate sensor (Courtesy of BEI Systron Donner Inertial Division)

Vibration of the drive tines causes them to act like the arms of a spinning ice skater, where moving them in causes the skater's spin rate to increase, and moving them out causes a decrease in rate. In the presence of tine vibration, an applied rotation rate about an axis parallel to the tines gives rise to a torque about the sensitive axis of the device that varies sinusoidally at the frequency of oscillation of the drive tines. The pick-up tines respond to this oscillating torque by moving up and down, out of the plane of the fork assembly, at the frequency of the drive tines. The motion of the pick-up tines is sensed, giving rise to an alternating electrical signal that is demodulated to produce a d.c. output proportional to the applied turn rate.

A further sensor that uses a quartz element is the Sagem Quapason gyroscope which has four quartz tines extending upwards from a common base. The advantage of this device is its ability to reduce unwanted cross-coupling from drive to sense channels [5].

7.3.3 Resonant ring MEMS gyroscopes

Vibrating ring structures have been successfully used to detect turn rates applied about an axis that is perpendicular to the plane of the ring using Coriolis force coupling between in-plane displacements. Such sensors have an advantage in that the ring structure maintains the drive and sense vibrational energy in a single plane. However, such devices do suffer from the drawback of having a relatively low vibrating mass, and hence exhibit a low scale-factor.

The initial work on this class of gyroscope involved the design of a vibrating element based on a gyroscope with a piezoceramic cylinder to sense the angular motion. The technology evolved into a device with a metal ring or disc resonator as the sensing element of the device, as shown in Figure 4.17 and described in Section 4.4.3. The design evolved through the use of silicon instead of metal [6–9].

An example of a MEMS implementation of this type of technology is the BAE Systems' silicon vibrating structure (SiVSG), which comprises a silicon ring supported by eight spokes that are radially compliant [10], as shown in Figure 7.10.

The silicon gyroscope creates and sustains a resonance in the structure through a combination of currents flowing through the metallic tracks on the surface of the ring and a magnetic field perpendicular to the plane of the sensor. This is analogous to an electric motor for the drive and a generator for the pick-off. The diameter of the ring is 6 mm, and the fundamental vibration mode of interest occurs at 14.5 kHz. The sensor chip is anodically bonded to a supporting glass structure, which has its thermal coefficient of expansion matched to that of silicon.

The sensing element has eight identical conducting loops that follow a similar path along metallic tracks on the surface of the silicon. These activation and pick-off circuits pass from the bond pad, along the top of one support leg, around one-eighth of the silicon ring, along the length on the next supporting leg and back to the bond pad. Each supporting leg has three conductors running along its length, one from each adjacent loop and between them a single conductor to minimise capacitive coupling. A ground plane is also created in this device by connecting to the silicon substrate.

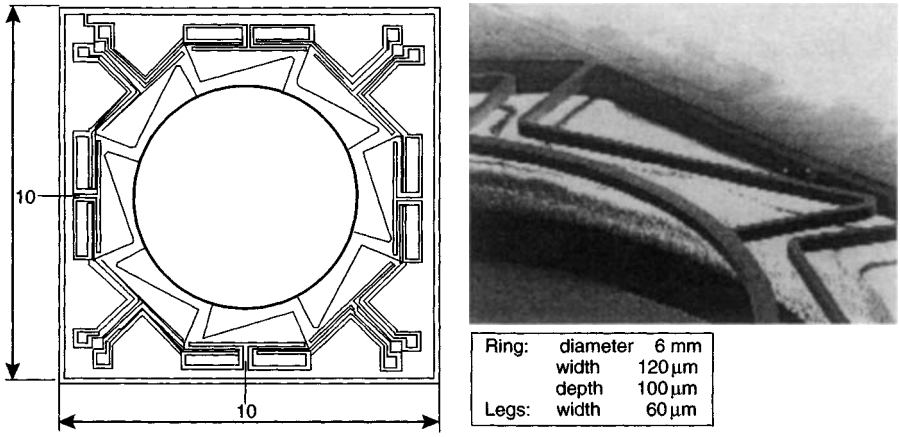

Figure 7.10 Silicon vibrating structure gyroscope sensitive element (Courtesy of BAE Systems)

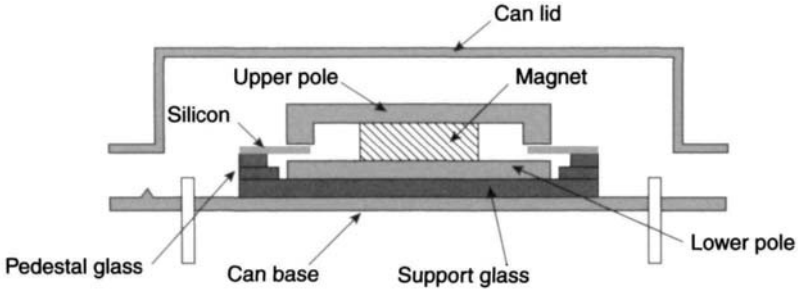

Figure 7.11 Cross-section of MEMS sensor (Courtesy of BAE Systems)

These conduction paths and a magnetic field, which is perpendicular to the plane of the silicon ring, form the drive and pick-off elements of the sensor. As usual, these transducers are arranged in pairs, 180° apart. The four transducers are the primary mode drive, the secondary mode drive, the primary mode pick-off and the secondary mode pick-off. A samarium cobalt magnet and a magnetic circuit, with two pole pieces, provide the magnetic field, which is confined to the size of the ring. The magnetic circuit maximises the magnetic field at the ring. A schematic of the layout is shown in Figure 7.11.

The sensing element has been designed so that the lowest order vibration mode is in excess of 5 kHz; this is whole-ring motion with respect to the mount. Consequently, this type of vibratory sensor is insensitive to the normal bandwidth of ambient vibratory motions experienced in many applications. Moreover, the design of the planar-ring structure is such that all of the vibratory motion is in one plane, whilst

being subjected to angular motion so there is no coupling of vibrations from one crystal plane to another. Hence, performance parameters such as frequency, modal-frequency split and Q are very stable over a wide temperature range.

The sensing element is operated in a closed loop mode to give high performance. The primary vibration mode is controlled by the primary drive loop to ensure that the vibration mode is at resonance; there is also an automatic gain control loop to control the magnitude of the displacement. When the sensor is subjected to angular disturbance, energy is coupled from the primary mode to the secondary mode. This motion is sensed by the secondary pick-off and this signal provides a measure of angular rate, that is, this would be an open-loop device architecture. However, in this design the secondary drive loop is used to null this motion, and this drive current provides the measure of the allied angular rate.

This form of feedback control aims to provide a constant modal pattern in the vibrating sensor during angular motion. This condition leads to improved linearity of the scale-factor and reduced bias. The combination of the automatic gain control (agc) loop and the secondary drive loop removes any 'Q' (quality factor) dependence from the scale-factor. This secondary loop is quite complex as it has two parts, a rate loop and a quadrature loop to null the quadrature motion in the resonator. The control of the so-called quadrature motion effects helps to minimise errors in the measurement of the applied angular motion about the input axis, resulting from frequency differences between the primary and secondary modes.

It is worth noting that in an open-loop configuration the scale-factor would have a Q^2 dependence.

It can be shown that the scale-factor is proportional to

$$\frac{\omega V_{\text{agc}}}{g_{\text{ds}} g'_{\text{p}} B^2}$$

The rate equivalent noise is given by:

$$\frac{K_1 f_{\text{n}} V_{\text{n}}}{g_{\text{d}} Q B^2 V_{\text{pd}}} \sqrt{\frac{4 f_{\text{BW}}^3}{3}}$$

where V_{pd} is the potential applied to the primary, V_{n} is the pick-off noise, V_{agc} is the potential of the agc loop, f_{n} is the resonant frequency ($\omega/2\pi$), f_{BW} is the output bandwidth, ω is the angular frequency, Q is the resonance quality factor, B is the magnetic field, K_1 is a term that includes the dimensions of the resonator and the mode shape (Bryan factor), g_{d} is the gain of the current amplifier, g_{ds} is the gain of the secondary amplifier and g'_{p} is the derivative of the gain of the pick-off amplifier.

This theory predicts that a sensor with a 40 Hz bandwidth will have an rms noise figure of the order of 0.2°/s, reducing to 0.025°/s for a sensor with a 0–10 Hz bandwidth.

This sensor has been developed for commercial applications by BAE Systems in conjunction with Sumitomo Precision Products Company Limited. The resulting device, fabricated using silicon, lends itself to batch production and is relatively inexpensive to produce. Whilst the sensor is suited to a wide range of

Table 7.2 SiVSG performance figures

Parameter	Value	Comments
Operating range (°/s)	±1000	
Turn-on bias stability (°/s)	<0.06	1σ
In-run bias stability (°/s)	0.05	1σ (0–30 min)
Scale-factor stability temperature sensitivity (%)	<±1	−40 to +85°C
Scale-factor linearity (% of FS)	<1	Input rates ±100°/s
Noise (°/s rms)	<0.5	0–45 Hz

commercial applications, particularly automotive, it has been designed to withstand the environments typical of military and space applications.

A summary of key performance figures is given in Table 7.2.

More recent developments have explored the possibilities for detecting angular rates applied about three mutually orthogonal axes using the Coriolis coupling between in-plane and out-of-plane displacements.

Along with BAE Systems, other corporations, such as Delphi[2] and QinetiQ are developing ring gyroscope components which stimulate the primary ring mode using electrostatic actuation techniques. Such implementations will offer significant advantages in the future, such as reduced power consumption, less complex assembly and a reduction in component size.

For multi-axis operation, the additional response of the ring owing to angular velocity applied about axes in the plane of the ring has been examined. In a similar manner to the single-axis ring resonator gyroscope, a carrier mode is maintained at constant amplitude. The carrier mode can be either an in-plane or an out-of-plane mode. When subject to a turn rate, Coriolis coupling is induced between the carrier mode and one or more response modes (in-plane or out-of-plane), depending on the axis about which the rate is applied. The magnitude of the induced response is proportional to the applied rate. The implementation of a number of concepts for sensors having two-axis and three-axis rate sensitivity is the subject of continuing research at the present time.

7.4 MEMS accelerometer technology

7.4.1 Introduction

As noted above, the use of silicon to make the precision micro parts of an accelerometer to measure the specific force being applied to an input axis is well established. The current state of development is that the entire sensor may be constructed entirely

[2] Originally developed in conjunction with Michigan University, USA.

from silicon, with the exception of the hermetically sealed case, which still tends to be metallic. Modern designs and precision micro-machining enable a precision sensor to consist of as few as five parts.

MEMS devices may be divided into two distinct classes, reflecting the manner in which acceleration applied to the case of the device is sensed:

- the displacement of a proof mass supported by a hinge or flexure in the presence of an applied acceleration, that is, a mechanical sensor using silicon components;
- the change in frequency of a vibrating element caused by the change in tension in the element as a result of the mechanical loading that occurs when the element is subjected to acceleration.

These MEMS devices are analogous to the pendulous open-loop and force-feedback accelerometers, and the vibrating-beam sensors described separately in Chapter 6.

As a general guide to the current state of technological development of these two distinct classes of inertial sensor, it may be considered that:

- pendulous types of MEMS accelerometer can provide acceleration measurements to an accuracy compatible with inertial (25 micro-g) or sub-inertial quality (1 milli-g);
- vibrating beam devices or resonant sensors tend to have a potentially higher accuracy capability approaching 1 micro-g.

7.4.2 Pendulous mass MEMS accelerometers

Both out-of-plane (sometimes known as z-plane) and in-plane pendulous devices have been developed and are in quantity production. Figure 7.12 shows a typical out-of-plane MEMS accelerometer in which a hinged pendulous proof mass, suspended by torsional spring flexures over a glass substrate, rotates when subjected to acceleration perpendicular to the plane of the sensor. One of the major attractions of this type of sensor is the versatility of the packaging, which enables planar mounting of the sensor.

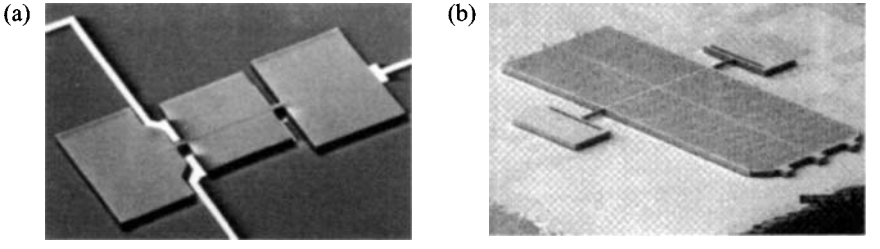

Figure 7.12 MEMS out-of-plane pendulous accelerometer (© The Charles Stark Draper Laboratory, Inc. All rights reserved. Reprinted with permission)

The device shown is a closed loop sensor having a dynamic range of 100 micro-g to $2g$. Both open and closed loop devices have been developed, and open-loop devices capable of measuring 100 000g are available.

Motion is detected by the change in the capacitance gap between the proof mass and the substrate using electrodes on an insulator substrate. Under a $1g$ acceleration, the change in angle of the proof mass is typically 70 μrad resulting in a change in the sense gap of approximately 3×10^{-8} m corresponding to a peak change in capacitance of 15 fF (fF = femtofarad; 1 fF = 10^{-15} F). Typical measurement ranges are from 100 micro-g to $15g$. To achieve this dynamic range, it is necessary to resolve motion of 3×10^{-12} m, or about 22.5 electrons charge change on the proof mass per carrier cycle.

Careful characterisation of this type of sensor is required as the scale-factor tends to decrease with increasing temperature [1]. The temperature dependence is systematic, and approximately linear, so it is easy to model and correct through a compensation routine.

Devices of this type, such as the Northrop Grumman SiAc™, have found broad application in a range of military applications, both tactical and inertial grade sensors having been produced. Similar devices have been produced through technical collaboration between The Charles Stark Draper Laboratory, Inc. and Honeywell. These are silicon devices which have been evaluated in extended range guided-munitions applications.

Figure 7.13 shows an in-plane (lateral) accelerometer which uses a comb finger construction as its sensing element. Acceleration is measured by detecting the change in capacitance across the comb fingers. This class of 'mechanical' sensor is much more sensitive to acceleration applied in the horizontal plane (as shown – or left to right) than in the orthogonal direction (or top to bottom).

Clearly, if a very small package is required then the use of a combination of these two types of pendulous accelerometer will give a very small and planar package that can sense acceleration along two or three axes. For example, the use of an out-of-plane sensing element and two lateral in-plane sensors, with their input axes orthogonal, will give a triple-axis sensor on a chip.

The analogue devices ADXL150 and ADXL250 are examples of this type of accelerometer. It is noted that the combination of in-plane and out-of-plane devices of the type described here allows systems capable of measuring acceleration along three mutually perpendicular axes to be constructed using a minimal volume package.

7.4.3 Resonant MEMS accelerometers

This class of sensors covers the general category of vibrating beam accelerometers which can be configured to sense accelerations acting in directions either in the plane of the sensor or perpendicular to it. Acceleration is sensed as a result of the change in the resonant frequency of beam oscillators under inertial loading of a proof mass, rather than the measurement of its displacement.

Out-of-plane resonant devices have been made by micro-machining at least one of the flexure members in a structure to form a piezoelectric resonator. The etching

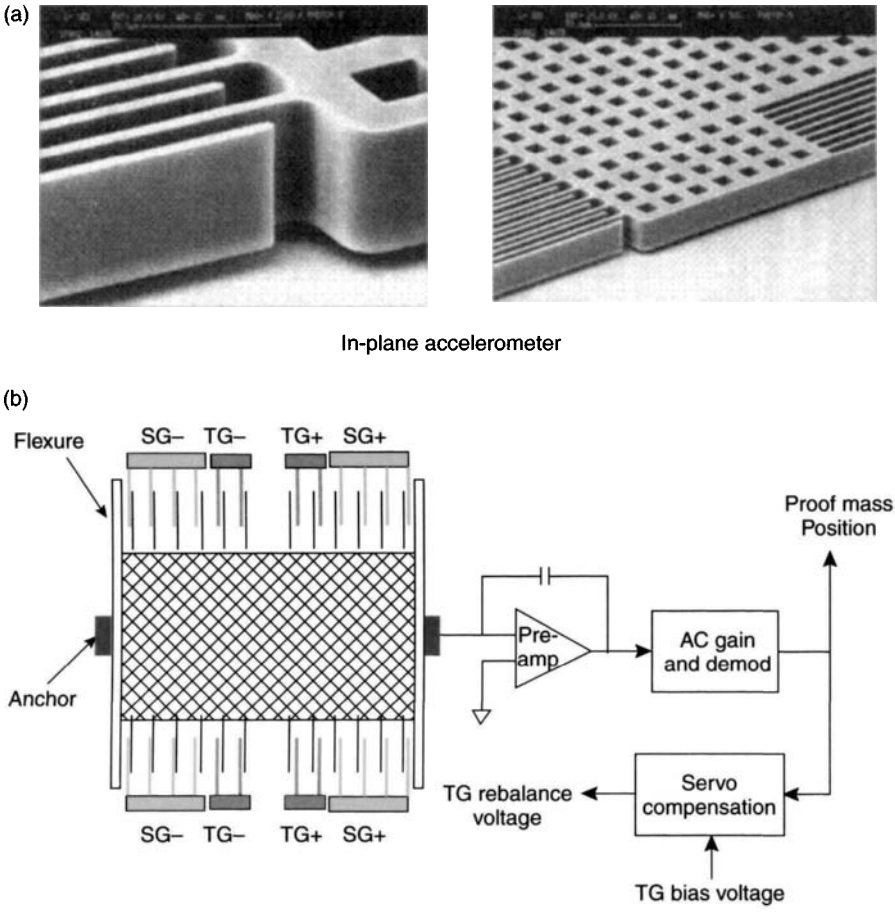

Figure 7.13 MEMS lateral in-plane accelerometer (© The Charles Stark Draper Laboratory, Inc. All rights reserved. Reprinted with permission)

of the structure is undertaken at positions where the resonator is calculated to have a zone, or zones, of high stress in its modal pattern. As the flexure element is distorted under the displacement of the proof mass the resonant frequency of the structure changes.

Both silicon and quartz devices have been fabricated. Figure 7.14 shows the in-plane (lateral) vibrating beam structure of a silicon oscillating accelerometer (SOA) developed by The Charles Stark Draper Laboratory, Inc. In this case the fundamental configuration is a monolithic vibrating tuning fork structure with a large silicon proof mass, which is driven electrostatically. The beams are loaded axially when an acceleration is applied in the plane of the vibratory motion (in the plane of the wafer) and the resonant frequency changes. Oscillator resonance and sensing is accomplished using a silicon comb drive structure as shown in the figure.

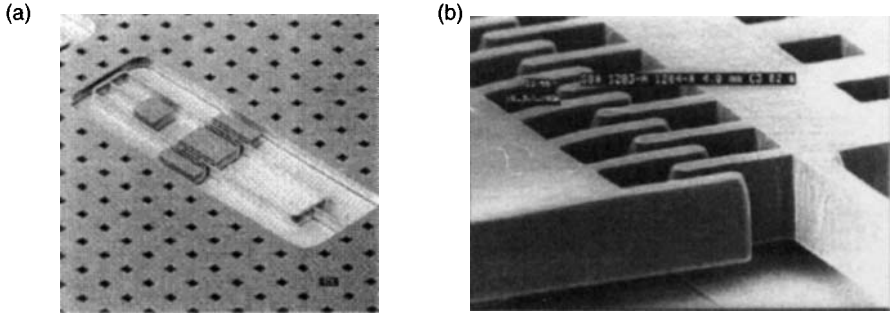

Figure 7.14 Silicon oscillating accelerometer (© The Charles Stark Laboratory, Inc. All rights reserved. Reprinted with permission)

The silicon oscillating accelerometer (SOA) MEMS accelerometer manufacturing process is silicon on glass; the silicon is perfectly elastic allowing very high precision frequency control and stability. The sensor is contained within a ceramic vacuum package, which provides high oscillator Q factor (typically $>100\,000$). For a device having a nominal oscillator frequency of 20 kHz and a scale-factor of 100 Hz/g, a frequency stability of 5 parts per billion yields a bias stability of 1 micro-g.

A device developed in France by ONERA[3] is of particular interest. This sensor has a mechanical isolating system that thermally isolates the vibrating beam from the mounting base and protects the sensing element from thermal stress caused by the differences in the thermal expansion coefficients of quartz and the case material. This class of accelerometer is capable of inertial-grade performance: accuracy of up to 1 micro-g bias stability has been reported.

7.4.4 Tunnelling MEMS accelerometers

This class of MEMS accelerometers is a recent development that offers significant enhancements over the devices described above that use read-out methods based on measurement of changes in capacitance. In this type of accelerometer the read-out has very high sensitivity and consequently offers better resolution, higher bandwidth and reduced size.

The control electrode deflects the cantilevered beam using an electrostatic force into a position known as the tunnelling position, a deflection of less than 1 μm. The device has a servo system that holds the beam in a position that maintains the gap between the tunnelling tip and the surface of the beam, and thereby maintains the tunnelling current, typically of the order of 1 nA. When an acceleration force is applied it attempts to move the beam and the servo system changes the applied potential at the electrode, and this change is a measure of the applied acceleration. A schematic view of this type of sensor is shown in Figure 7.15. The construction uses

[3] Office National d'Etudes et de Recherches Aérospatiales.

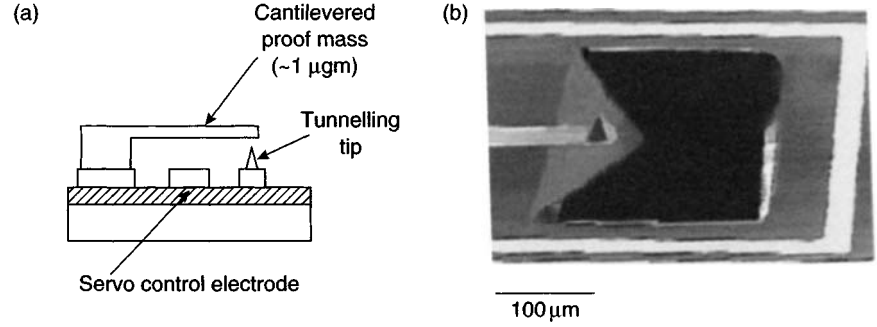

Figure 7.15 Schematic of a MEMS tunnelling accelerometer (© The Charles Stark Draper Laboratory, Inc. All rights reserved. Reprinted with permission)

a structure with low resonant frequency proof mass cantilever beams with a mass of the order of 1 μg and read-out circuits with sub-Angstrom resolution.

This class of sensors is designed to have a resolution in the nano-g regime. However, the dynamic range is relatively modest at approximately 10^6, so the maximum input acceleration is in the 1 milli-g range.

7.4.5 Electrostatically levitated MEMS accelerometers

There have been many diverse studies and developments aimed at removing the constraints imposed by the elastic restraint and non-linear response of supporting mechanisms. The dynamically tuned gyroscope (Section 4.2.6) and the mass unbalance sensor (Section 6.5.4) are two particularly successful devices. However, the sensing element is only free over a very small angle. Novel gyroscopes such as the nuclear magnetic resonance device (Section 4.5.1) and the electrostatically suspended sensor (Section 4.6) are other examples aimed at very specialised applications.

A new approach involving MEMS technology and electrostatic levitation aims to produce a high performance accelerometer with high sensitivity, very accurate resolution and an easily adaptable response bandwidth, without modification to the structure. Additionally, the use of levitation of a small proof mass could ease some of the demanding fabrication tolerances. As with all of these novel approaches, there is a shift in the design difficulty and in this case it is to the control loop which becomes complex. However, with modern computational techniques and electronic systems this should not be an insurmountable problem.

This new approach has a small sphere 1 mm diameter with a mass of 1.2 mg suspended in an electrostatic field. The position of this sphere is sensed by changes in capacitance and a closed loop servo system maintains the position of the sphere by

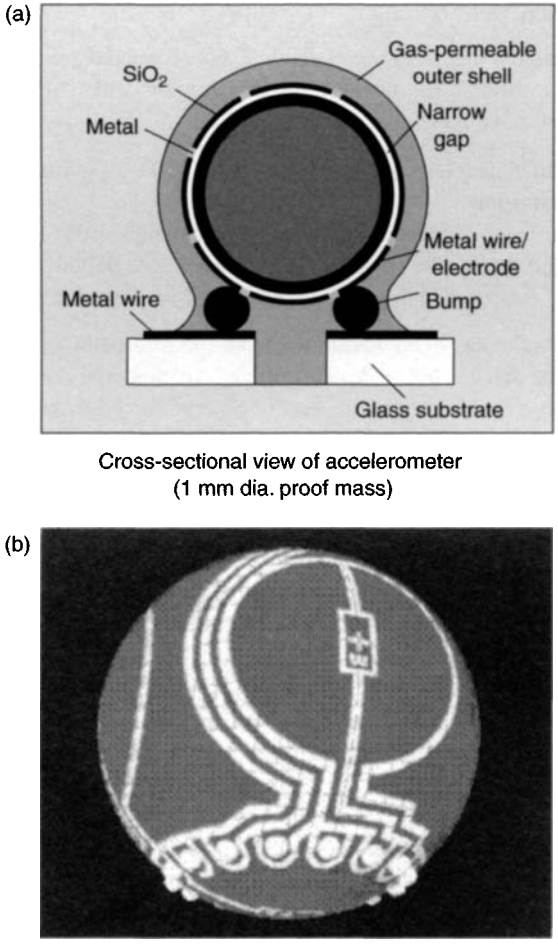

Figure 7.16 Levitation accelerometer (© The Charles Stark Draper Laboratory, Inc. All rights reserved. Reprinted with permission)

controlling the electrostatic force on the sensing element. A schematic representation of the sensor is shown in Figure 7.16.

The gap between the sphere and the outer shell is formed by removal of a sacrificial layer of polycrystalline silicon, which is etched through the outer shell structure.

An alternative approach using a levitated disc is under consideration at the University of Southampton in the United Kingdom [11]. This class of technology with a levitated spinning mass sensing element could lead to a very capable inertial sensor.

This type of sensor is aimed at the measurement of micro-gravity measurements in space and is expected to have a noise value in the region of 40 micro-$g/\sqrt{\text{Hz}}$.

7.4.6 Dithered accelerometers

There has long been a desire to use a single class of inertial sensor to provide all of the inertial measurements for an inertial measurement unit (IMU). Some examples of approaches that have had some success include:

- use of multiple accelerometers, but this is difficult owing to the real-time processing required;
- use of mass unbalanced tuned rotor gyroscopes, which also requires quite complex processing and the sensor package is quite large; see Section 6.5.4;
- use of multi-sensors, which again are not small sensors; see Section 6.5.

A novel technique has been developed from the multi-sensor approach to enable angular rate to be sensed by an accelerometer. In this sensor, the three opposing pairs of monolithic resonating beam accelerometers are dithered about an axis on a vibrating structure. Acceleration applied about the input axes is sensed from the change in resonant frequency of the vibrating beams in the device. The angular motion is sensed from synchronous demodulation of the Coriolis force acting on the accelerometers.

This device has been developed in the form of the micro-machined silicon Coriolis Inertial Rate and Acceleration Sensor (μSCIRAS) [13].

7.5 MOEMS

A new approach to micro-machined sensors is micro-opto electromechanical systems (MOEMS). This class of technology offers a true solid-state sensor with an optical readout, so the limitations in performance of MEMS devices using capacitative techniques for measuring small displacements are eliminated.

Various optical pick-off techniques are current topics of research. These are either interferometric approaches, which offer low noise and high resolution, or attenuation methods, involving the interruption of a light beam from a diode. These approaches, or others, may be adapted as the characteristics and origin of the noise are understood, and fully characterised. Another important aspect of an optical read-out is the installation and alignment/harmonisation of the optical source and its detector; particular considerations are low-cost installation and maintainability.

7.6 Multi-axis/rotating structures

The approach of mounting in-plane sensors on a rotating ceramic mounting block and using demodulation techniques to extract the multi-axis inertial data from a reduced number of sensors, has enabled a considerable size reduction in multi-axis systems to be achieved. Off-axis sensors may be used for measuring orthogonality.

The use of the more modern in-plane and out-of-plane sensors is likely to lead to a further reduction in IMU size and make the need for a rotating structure redundant for many applications.

7.7 MEMS based inertial measurement units

A number of projects are underway to produce multi-axis sensors on a chip, which will provide estimates of angular rate as well as linear acceleration. Examples include the combination of two in-plane and one out-of-plane MEMS sensors on a single chip. Such approaches offer many advantages including:

- ease of manufacture;
- a vast reduction in volume;
- negligible power consumption;
- ability to carry out a complete characterisation of the unit in a single operation.

7.7.1 Silicon IMU

The 'Draper' laboratory has reported one chip that has two tuning fork gyroscopes and one out-of plane gyroscope. A complementary chip with three accelerometers has been produced; this integrated sensor also has two in-plane accelerometer sensors and a single out-of-plane pendulous device. The resulting inertial measurement unit has a volume of about 3.3 cm^3 [1]. However, further work is required before a high performance IMU is available.

BAE Systems has developed a silicon-sensor based IMU for a number of applications [12]. The IMU has three sensing axes, which are in a right-handed orthogonal set. Each sensor axis has an associated set of devices to sense angular rate about that axis, acceleration along that axis and temperature of the sensors. An exploded view showing the layout of the components is shown in Figure 7.17.

This IMU has been designed to operate in an environment that is subjected to high angular rates. The inertial sensors are arranged on the edges of a cube to form

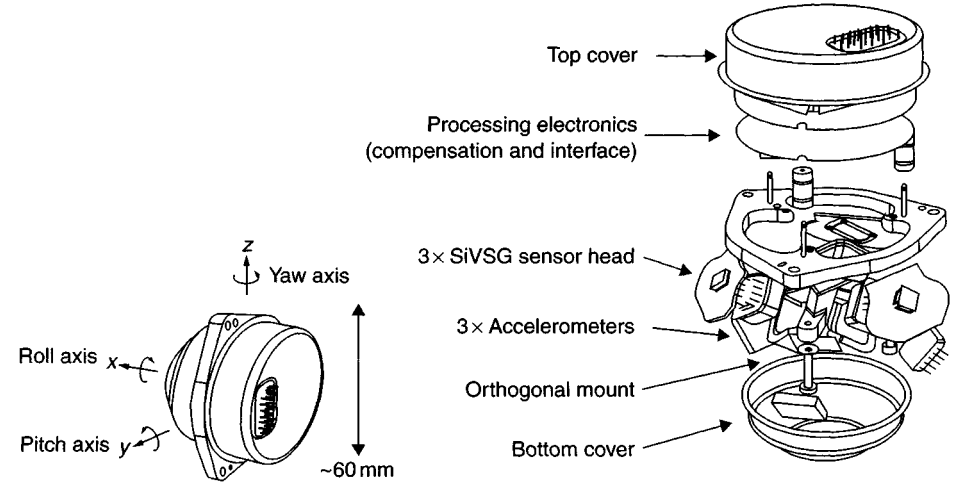

Figure 7.17 SiIMU® (Courtesy of BAE Systems)

a right-handed orthogonal set of axes. This axis system is rotated away from the vertical; however, the relative orientations of the sensors with respect to each other are not skewed. This configuration has the input axes of all sensors at 54.73° to the vertical and is equally spaced at 120° to each other in the horizontal plane.

A direction cosine matrix is used to convert the sensed motion by each of the sensors into a body reference frame. This approach is necessary as no one sensor is aligned with the body axis reference frame in this configuration of sensor axes.

This skew or rotated axis configuration enables

- the x-axis (of the vehicle) to sense up to $\sqrt{3}$ times the maximum input angular rate of the gyroscope, when the input rates about the other two orthogonal body axes are zero; similarly for the accelerometer;
- common mode errors, such as sensor bias, to be magnified by $\sqrt{3}$ for the x-axis, but reduced for the orthogonal axes.

The downside of this configuration is that if the vehicle containing the IMU is subjected to the same maximum rates simultaneously, then this configuration will require sensors with a higher maximum rate capability than would be needed for the non-rotated cluster.

One of the aspects for achieving high navigational data capability from these small sensors is to undertake characterisation and modelling of the sensors. This type of sensor requires equipment that allows application of maximum temperature, acceleration and rates to at least two independent axes. Hence, a single-axis rate table is inadequate, as scale-factor errors and misalignments need to be observed independently; therefore dual-axis rate tables are used in the characterisation.

This IMU compensates for the following systematic errors:

- sensor bias;
- sensor scale-factor errors;
- 'g-dependent' bias of the silicon gyroscopes;
- misalignment of axes from harmonisation errors and non-orthogonality;
- size effect.

The compensation routine for compensating the above errors runs in real time. This leads to a unit with a run-to-run bias of 200°/h (1σ) and 'g'-dependent bias of 7°/h/g (1σ). The corresponding performance for the measurement of acceleration is 20 milli-g (1σ).

7.7.2 Quartz IMU

The quartz rate sensor (QRS), described in Section 7.3.2.2, together with a vibrating quartz accelerometer have been built into an IMU; the Systron Donner Digital Quartz IMU (DQI). This is a solid-state, six-degree of freedom inertial measurement system that provides measurements of angular rate and linear acceleration about three orthogonal axes [4]. The integrated unit combines the inertial sensor assembly, the inertial sensor assembly electronics and a processor in which digital filtering and compensation algorithms are implemented.

Figure 7.18 BEI C-MIGITS™ III miniature INS/GPS integrated system (Courtesy of BEI Systron Donner Inertial Division)

The inertial sensor assembly is machined out of a single aluminium block to form a cube, and is designed to eliminate structural resonances that would coincide with any of the sensor drive modes. To further eliminate coupling between the individual sensors, each sensor operates at a unique drive frequency. One of the advantages of using quartz sensors is the stability of this material, which allows each gyroscope to be produced to a known frequency which can be accurately maintained.

MIGITS™ is a family of products for applications requiring guidance, navigation and control. The C-MIGITS™ III system, shown in Figure 7.18, is a compact and lightweight system that contains the Systron Donner DQI and a commercial GPS receiver. The inertial system and GPS measurements are combined using a tightly coupled integration architecture; discussed separately in Section 13.7.

7.8 System integration

An array of MEMS sensors may be integrated into a single chip to provide multiple independent measurements of inertial motion. A direct advantage of this class of technology is that the sensors may be integrated directly to the electronic control circuits, in an applications specific integrated circuit (ASIC) configuration, in a single

hermetically sealed package. The logic control may be achieved by the use of field-programmable gate arrays.

The characteristics of the MEMS devices tend to be of a form that is readily corrected leading to a sub-system that can be hard mounted in a vehicle. These devices have been used in cannon-launched projectiles that experience many thousands of 'g' during the launch of the weapon. The power requirements are modest and compatible with normal electronic circuitry.

MEMS devices are ideal for integration with other navigation systems, both in terms of complementary error characteristics and small size with rugged operational characteristics.

7.9 Summary

MEMS sensors have developed substantially over the last 15 years in many respects. A number of new approaches have been very successful and this has led to high performance devices. Advances in the micro-machining techniques have provided a substantial enhancement to the technology, leading to substantial cost reduction. As the technology has advanced there has been a greater understanding of the cause and effects of the error mechanisms and the need for a close integration between the sensing element and the electronic control circuits.

The performance of MEMS devices has increased by many orders of magnitude over a decade or so, owing to successful development projects. Consequently, MEMS accelerometers and gyroscopes are capable of providing inertial-grade measurements of acceleration and angular motion for long-range navigation systems.

Techniques have been demonstrated that enable the sensing devices of an inertial measurement unit to be fabricated on a single chip for lower-grade requirements. Methods for characterisation and compensation of systematic errors are proven and have been applied successfully to a range of systems. However, there is still scope for further improvement!

There is optimism that further enhancements are possible as a greater understanding is reached of the effects that geometry, size, packaging and interference from electronic circuits have on the performance of these miniature devices. It would be advantageous to improve the turn-on to turn-on repeatability, and reduce the initial transient response particularly for rapid reaction applications. Other performance areas where there is scope for improvement include: reduction in noise, improved fabrication precision, improved electronic control and reduced sensitivity to packaging.

The development of MOEMS devices is likely to lead to a further enhancement in performance owing to the true solid-state nature of these devices.

References

1 BARBOUR, N.: 'Inertial navigation sensors', NATO RTO Lecture Series-232, 'Advances in Navigation Sensors and Integration Technology', Oct. 2003

2 BARBOUR, N., ANDERSON, R., CONNELLY, J., *et al.*: 'Inertial MEMS system applications', NATO RTO Lecture Series-232, 'Advances in Navigation Sensors and Integration Technology', Oct. 2003
3 GAIßER, A., FRECH, J., SCHUMACHER, A., *et al.*: 'Evaluation of DAVED – microgyros realised with a new 50 μm SOI-based technology'. Presented at DGON symposium, *Gyro Technology*, Stuttgart, 2003
4 BAKER, G.: 'Quartz MEMS GPS/INS technology developments'. Presented at DGON symposium, *Gyro Technology*, Stuttgart, 2003
5 LÉGER, P.: 'Quapason – a new low cost vibratory gyroscope'. Presented at DGON symposium, *Gyro Technology*, Stuttgart, 1996
6 ELEY, R., FOX, C.H.J., and McWILLIAM, S.: 'The dynamics of a vibrating-ring multi-axis rate gyroscope', *Proc. Institution of Mechanical Engineers*, 2000, **214**, Part C
7 ROURKE, A.K., FOX, C.H.J., and McWILLIAM, S.: 'Development and testing of novel, multi-channel vibrating structure rate sensor'. Presented at DGON symposium, *Gyro Technology*, Stuttgart, 2003
8 FOX, C.H.J., ROURKE, A.K., ELEY, R., FELL, C., and McWILLIAM, S., 'Multi-channel and multi-axis inertial sensor concepts based on vibrating structures'. Presented at SPIE conference, *Smart Structures and Materials*, San Diego, CA, March 2003
9 ROYLE, C.M., and FOX, C.H.J.: 'The mechanics of an oscillatory rate gyroscope with piezoelectric film actuation and sensing', *Proc. Institution of Mechanical Engineers*, 2001, **215**, Part C
10 FOUNTAIN, J.R.: 'Characteristics and overview of a silicon vibrating structure gyroscope', NATO RTO Lecture Series-232, 'Advances in Navigation Sensors and Integration Technology', Oct. 2003
11 HOULIHAN, R.: 'Modelling of an accelerometer based on a levitated proof mass', *Journal of Micromechanics and Microengineering*, 1992, **13** (4), pp. 495–503
12 FOUNTAIN, J.R.: 'Silicon IMU for missile and munitions applications', NATO RTO Lecture Series-232, 'Advances in Navigation Sensors and Integration Technology', Oct. 2003
13 HULSING, R.: 'MEMS Inertial rate and acceleration sensor,' ION National Technical Meeting, CA, January, 1998